1 Introduction

Alzheimer's disease (AD) is a debilitating medical condition that affects one in eight people over 65 years of age [1]. However, precise details of the mechanism that causes AD are largely unknown. Here we build a graph theoretic model that demonstrates the importance of symmetry of the cerebral arterial tree to the proliferation of AD.

1.1 Medicine

Extracellular space in the brain contains interstitial fluid (ISF) which is produced by the blood and by-products of cell metabolism. The extracellular spaces within the walls of cerebral blood vessels referred to as *basement membranes* represent the perivascular pathways along which ISF drains out of the brain [2, 3, 4]. Figure 1 depicts perivascular drainage of Aβ along basement membranes.

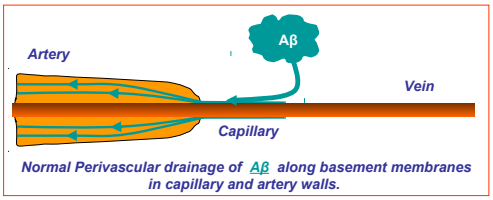

Figure 1

The walls of cerebral capillaries consist of one fused layer of the basement membrane which is approximately 150 nm in thickness.

Alzheimer's disease is the most common dementia - characterised by serious and progressive cognitive decline and appears to be due to a failure of elimination of amyloid-β (Aβ) from the brain. Aβ is a normal by-product of cell metabolism produced at all ages [2].

One mechanism for the removal of Aβ from the brain parenchyma is perivascular drainage, by which Aβ within ISF enters the capillary basement membranes draining to the walls of arteries towards the surface of the brain. With ageing and certain genetic background soluble Aβ is not eliminated from the brain and it is deposited in the walls of blood vessels as cerebral amyloid angiopathy (CAA) [4][2]. In Figure 2 the deposition of Aβ is shown in red.

The deposition of Aβ in the perivascular spaces in the blood vessel walls can cause a further blockage of the ISF drainage pathways resulting in an alteration of the composition of ISF in the brain parenchyma. This change in biochemical composition of the ISF leads to nerve cell death and Alzheimer's Disease. [4].

CAA is most prominent in the occipital, temporal and frontal lobes and least prominent in the parietal lobe and cerebellum. In particular, the leptomeningeal and cortical arteries are particularly prone to CAA whereas CAA is very rare in capillaries [5]. One possible reason for the differing expected degrees of CAA could be the differing topology and symmetry of the cerebral arterial tree. In order to test this hypothesis we consider a graph theoretic model of CAA and therefore need to make some relevant definitions from graph theory.

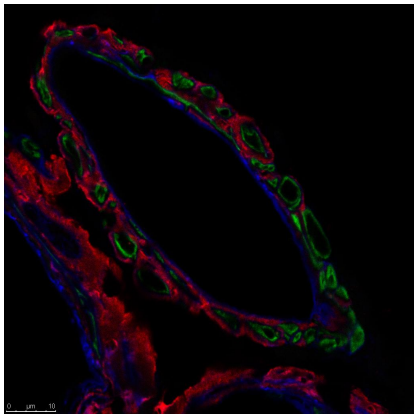

Figure 2: CAA in a leptomeningeal artery.

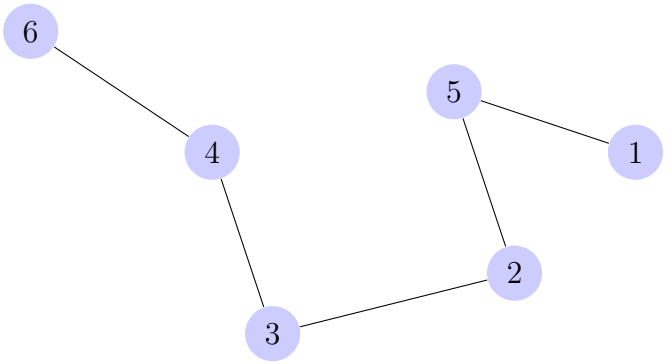

Figure 3

1.2 Graph Theory

The references for this section are [6] and [7]. Graph Theory has been an established area of discrete mathematics since 1736 when Euler solved the famous question regarding the bridges of Königsberg. More recently, in the 1940s and 50s Erdős and Rényi laid the foundations of the theory of random graphs seeking to answer fundamental questions about the nature of "most" graphs. Random graphs have been studied for their own sake and have been used to model a diverse set of real-world networks from the world wide web to the metabolism of *E. coli* [8]. Recently the advent of the world wide web and the accompanying cheap and powerful computational power has led to a re-emergence of random graph theory under the guise of "Network Science".

An simple undirected graph, G, is a pair $G = (V(G), E(G))$ where $V(G)$ is the a set of vertices or nodes of the graph and $E(G)$ is the set of edges of G. Each edge $e \in E(G)$ has two endpoints $u, v \in V(G)$ and we say that if $e = e_{u,v}$ then u and v are *adjacent* and that $endpoints(e) = \{u, v\}$. We do not allow more than one edge between a pair of vertices or loops which are edges e such that $endpoints(e) = \{u\}$. The degree of any vertex v is the number of edges e such that $v \in endpoints(e)$.

A tree, T, is a graph such that the shortest path between any pair of vertices $u, v \in V(T)$ is unique. For example the graph in Figure 3 is a tree.

A *random recursive tree* (RRT), T, with vertices $V(T) = \{v_1, \ldots, v_n\}$ is a labelled, rooted tree obtained by assigning a root vertex v_1 then adding $n-1$ vertices one by one such that each new vertex is joined by an edge to a randomly and uniformly chosen existing vertex. A random recursive q-ary tree is a labelled, rooted tree built in the same way as a random recursive tree except each new vertex is attached uniformly at random to an existing vertex that has outdegree

less than q [7]. We say that RRTs and random recursive q-ary trees are *increasing* trees.

Given an increasing tree T_n on n vertices labelled by the function $\phi : V(T) \to \{1, 2, \ldots, n\}$ and a vertex $v \in V(T)$ then we can consider $\tilde{T}_v$ which is the induced subtree with vertices, $v_i \in B(v)$ such that $\phi(v_i) \geq \phi(v)$.

Given some tree T we can formally measure how *symmetric* that tree is by calculating the number of permutations of the vertices of that graph which preserves adjacent vertices. We call the set of all these permutations, $Aut(T)$, the *automorphism group* of T and the number of allowed permutations, $|Aut(T)|$ is the size of the automorphism group.

Example 1.1. Consider the following increasing tree T_{14} with 14 vertices.

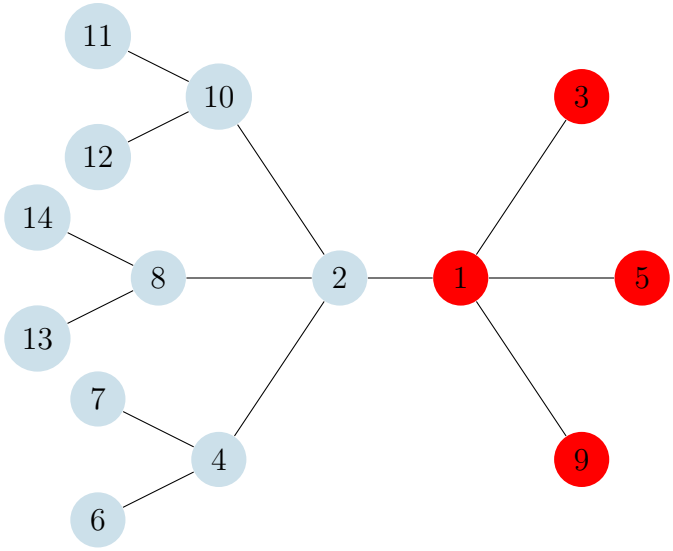

Figure 4

The red vertices in Figure 4 indicate an induced subtree $\tilde{T}_{v_1}$. We can permute the vertices v_3, v_5 and v_9, for example the following is a valid permutation of these vertices.

$$3 \to 5$$
$$5 \to 3$$
$$9 \to 9$$

Note that after the above permutation all three vertices remain adjacent to v_1. There are $3! = 6$ distinct such permutations. The blue vertices in Figure 4 highlight an extended symmetric induced subtree, $\tilde{T}_{v_2}$. We can permute any of the pairs $\{v_6, v_7\}, \{v_{11}, v_{12}\}$ and $\{v_{13}, v_{14}\}$ and we can permute the longer branches. For example the following is a valid (adjacency preserving) permutation:

$$4 \to 8$$
$$6 \to 13$$
$$7 \longrightarrow 14$$
$$8 \to 4$$
$$13 \to 7$$
$$14 \to 6$$

Where every other vertex is fixed. There are X possible valid permutations of the blue vertices, therefore $|Aut(T_{14})| = 6 \times X = 6X$

1.2.1 Anatomical Data

In order to build an effective model we require anatomical data such as the expected length and radii of arterial vessels and the expected number of branching points.

Note that 98% of branching in the cerebral cortex is bifurcation and we expect approximately 300 branching points [9].

Murray's principle of minimization of operational cost states that the cost of operation of physiological systems tends to a minimum. One consequence of Murray's principle is referred to as Murray's law which states that for 2 daughter branches d_1 and d_2 from a common parent arterial vessel, p:

$$r_p^3 = r_{d_1}^3 + r_{d_2}^3$$

where r_p is the radius of p and r_{d_1}, r_{d_2} are the radii of d_1 and d_2 [10]. Experimental evidence has shown that Murray's law is a good approximation for arterial vessels [11, 12].

Murray's law describes the relationship between particular vessels which can be thought of as *cylinders*. However, recall that our goal is to model the cerebral perivascular pathways which can be thought of as *annular prisms*. Therefore we will adjust Murray's law to describe the relationship between parent and child annular prisms. Since the notion of radius is more complicated for an annular prism it is necessary to reformulate Murray's law in terms of cross-sectional area.

We assume that the width of the perivascular space, ϵ is the same for any vessel from capillary to artery. So let he parent vessel have radius $r_p = r'_p + \epsilon$ and the two daughter vessels have radii $r_{di} = r'_{di} + \epsilon$. The relationship between the cross-sectional area, A_X of any vessel and the radius, r_X of that vessel is given by the formulae:

$$\begin{aligned} A_X &= \pi((r'_X + \epsilon)^2 - r'^2_X) \\ &= \pi(\epsilon^2 + 2\epsilon r'_X) \\ r'_X &= \frac{A_X - \pi\epsilon^2}{2\epsilon\pi} \\ r_X &= \frac{A_X - \pi\epsilon^2}{2\epsilon\pi} + \epsilon \\ &= \frac{A_X + \pi\epsilon^2}{2\epsilon\pi} \end{aligned}$$

By combining the above equations we find that the cross-sectional area of the parent vessel, A_p, is given by:

$$\begin{aligned} A_p &= \pi(\epsilon^2 + 2\epsilon r_p) \\ &= \pi\left(\epsilon^2 + 2\epsilon(r_{d_1}^3 + r_{d_2}^3)^{\frac{1}{3}}\right) \\ &= \pi\left(\epsilon^2 + 2\epsilon\left(\left(\frac{A_{d_1} + \pi\epsilon^2}{2\epsilon\pi}\right)^3 + \left(\frac{A_{d_2} + \pi\epsilon^2}{2\epsilon\pi}\right)^3\right)^{\frac{1}{3}}\right) \end{aligned}$$

where A_{d_1} and A_{d_2} are the cross-sectional areas of the two daughter vessels.

2 Method

In this section we will describe the program we built using the numerical modelling program *matlab* [13] which replicates CAA. This program has four constituent parts:

(i) Generate a random recursive q-ary tree, T_n^q on n nodes.

(ii) Calculate $|Aut(T_n^q)|$.

(iii) Dynamically remove edges of T_n^q according to a predetermined probability model.

(iv) Record the time, $\tau_{\frac{1}{2}}$, to remove half of the edges from T_n^q which we think of as the "half-life" of the process.

This program was then run 50 times and we investigated the relationship between $|Aut(T_q^2)|$ and $\tau_{\frac{1}{2}}$.

In accordance with the anatomical survey paper by Cassot *et al.* discussed in Section 1.2.1 we set $n = 300$ and $q = 2$. We used the graph isomorphism program *nauty* [14] to calculate the size of the automorphism group of each tree.

The dynamic process of edge removal can be defined as follows. At time $t = 0$ we set $T(0) = T_{300}^2$ our randomly generated binary tree. At time $t = 1, 2, \ldots$ for every edge $e \in E(T(t-1))$ there is some probability $0 < P \leq 1$ that e is removed. If edge $e = e_{uv}$ is removed then we also remove the induced subtree $\tilde{T}_u$ to form $T(t)$. In medical terms the removal of an edge corresponds to a level of CAA in the relevant vessel's basement membrane which prevents perivascular drainage along that edge. Our model includes the removal of the induced subtree because a blockage in some vessel V will render useless all daughter vessels of V.

We made the assumption that probability P depends on the concentration of Aβ in the basement membrane. In order to calculate the concentration of Aβ we must make further morphological definitions. Recall that we associate each edge in T_{300}^2 with an annular prism from Section 1.2.1. We define the cross-sectional area of a leaf edge (capillary) to be one and then every other edge's cross-sectional area can be derived from Murray's law adjusted for annular prisms. For simplicity we define the length of every vessel to be one so now we can make sense of the volume, $Vol(e)$, of any edge $e \in E(T_{300}^2)$.

We define the total initial volume to be $Vol_I = \sum_{e \in E(T(0))} Vol(e)$ and the total current volume to be $Vol_C(t) = \sum_{e \in E(T(t))} Vol(e)$. A$\beta$ is produced at an approximately constant rate over our life time [3]. We assume that perivascular drainage is able to remove a constant quantity of $A\beta$ even in the face of adversity (the blockage of certain routes) and we initially set the concentration, $C(0) = 1$ and subsequently:

$$C(t) = \frac{Vol_I}{Vol_C(t)}.$$

We can now define $P = p.C(t)$ where $0 < p < 1$ if $pC(t) < 1$ and $P = 1$ if $p(C(t)) \geq 1$.

3 Results

We generated 50 random recursive binary trees.

A relatively crude way of estimating the resilience of a tree to the deletion process outlined in Section 2 is to calculate the time, $\tau_{\frac{1}{2}}$, it takes for half the vertices to be removed. In the brain this would be a catastrophic loss of perivascular pathways and reflects the advanced stages of CAA.

We generated 50 random recursive binary trees $\mathcal{T}$ and for each $T_{300}^2 \in \mathcal{T}$ we calculated $|Aut(T_{300}^2)|$. We calculated the median, ϕ, of the automorphism group sizes and split $\mathcal{T}$ into two subsets.

$$(T_1) = \{T_{300}^2 | Aut(T_{300}^2) < \phi\} \text{ and } (T_2) = \{T_{300}^2 | Aut(T_{300}^2) \geq \phi\}$$

We then calculated the means μ_i of the $\tau_{\frac{1}{2}}$ such that $T \in \mathcal{T}_i$ for $i = 1, 2$. The results are shown in Figure 5.

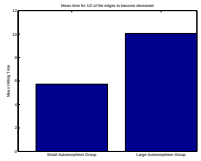

Figure 5: $\tau_{\frac{1}{2}}$.

For further corroboration we also defined $\tau_{\frac{2}{3}}$ and the corresponding μ_1' and μ_2'.

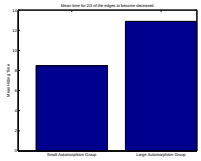

Figure 6: $\tau_{\frac{2}{3}}$.

The results show that the trees that were generated with a larger automorphism group had larger half and two thirds lives than the trees generated with smaller automorphism group.

3.1 Interpretation of results

To understand the medical relevance of these results note that large $\tau_{\frac{1}{2}}$ means that it took longer for half of the vessels to be removed so the degree of CAA was less severe. Our results suggest that a cerebral vascular structure that is highly symmetric (has a large automorphism group) is more *robust* to CAA.

High levels of symmetry have been shown to be advantageous in other networks. For example Song *et al.* create a mathematical model to study the evolution of a biochemical annotation network. They show that a fractal network (a graph with a high level of symmetry) is more robust i.e. the removal of many nodes has minimal effect on the shortest paths [15].

To gain some intuition as to why this is the case consider the following extreme example. Let T_1 be the complete tree on 15 vertices and let T_2 be a line of 15 vertices as seen in Figure 7. Notice that $|Aut(T_1)| = BIG$ and that $|Aut(T_2| = 2$ so T_1 is much more symmetric than T_2.

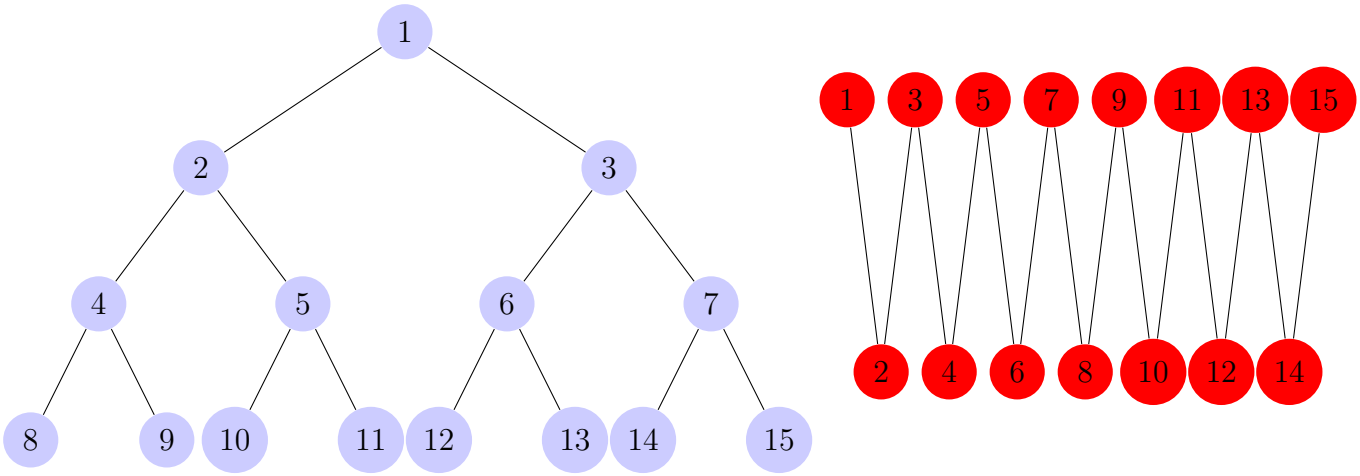

Figure 7: T_1 and T_2

If we remove an edge at random from T_1 and also remove the induced subtree adjacent to that edge the expected number of edges removed is:

$$1\frac{8}{14} + 3\frac{4}{14} + 7\frac{2}{14} = \frac{12}{7} \tag{1}$$

If we remove an edge at random from T_2 and also remove the induced subtree adjacent to that edge the expected number of edges removed is:

$$\frac{1}{14}\sum_{k=1}^{14} k = \frac{15}{2} > \frac{12}{7} \tag{2}$$

One could argue that our results were the result of weak assumptions regarding concentration, however we yielded a similar result with a simplified experiment. We built 50 random recursive binary trees $\mathcal{T}$ in the same way and set P to be constant rather than a function of concentration. We split $\mathcal{T}$ into $\mathcal{T}_1$ and $\mathcal{T}_2$ and found the mean hitting times μ_1 and μ_2. Again we found that $\mu_1 < \mu_2$.

4 Conclusions and Further Directions

In order to improve the accuracy of our model we could make several modifications. Firstly, Ambrose has shown that the brain undergoes angiogenisis (the creation of new arterial vessels) which could be reflected in the model by adding edges at random. Further we could modify the deletion process by going from a model in which an edge either exists or does not to a model in which each edge allows a variable flow which decreases at random. We could also attempt to reflect the fact that modelling the basement membranes as annular prisms does not take into account the tortuous routes of perivascular drainage. Finally, we could also model the stiffening of arteries over time by introducing a radial function that monotonically decreases.

We have demonstrated that it is likely that there is correlation between symmetry of the cerebral vasculartureand lower risk of proliferation of CAA. Further evidence of this correlation could be found by examining the relationship between highly symmetric areas of the brain and the extent to which those areas are affected by CAA.

References

[1] F. Mangialasche *et al.*, Lancet neurology **9**, 702 (2010).

[2] R. Weller, M. Subash, S. Preston, I. Mazanti, and R. Carare, Brain Pathology **18**, 253 (2008).

[3] R. O. Weller, D. Boche, and J. A. Nicoll, Acta neuropathologica **118**, 87 (2009).

[4] D. Schley, R. Carare-Nnadi, C. Please, V. Perry, and R. Weller, Journal of Theoretical Biology **238**, 962 (2006).

[5] S. Preston, P. Steart, A. Wilkinson, J. Nicoll, and R. Weller, Neuropathology & Applied Neurobiology **29**, 106 (2003).

[6] B. Bollobás*Modern graph theory* Vol. 184 (Springer Verlag, 1998).

[7] F. Bergeron, P. Flajolet, and B. Salvy, *Varieties of increasing trees* (Springer, 1992).

[8] H. Jeong, B. Tombor, R. Albert, Z. N. Oltvai, and A.-L. Barabási, Nature **407**, 651 (2000).

[9] F. CASSOT, F. LAUWERS, C. FOUARD, S. PROHASKA, and V. LAUWERS-CANCES, Microcirculation **13**, 1 (2006).

[10] C. D. Murray, The physiological principle of minimum work: I. the vascular system and the cost of blood volume., 1926.

[11]

[12] M. Zamir, The Journal of General Physiology **67**, 213 (1976), http://jgp.rupress.org/content/67/2/213.full.pdf+html.

[13] *MATLAB* (The MathWorks Inc., Natick, Massachusetts, 2010).

[14] *nauty* .

[15] C. Song, S. Havlin, and H. A. Makse, Nature Physics **2**, 275 (2006).